Potent Inhibitors of HIV-1 Integrase Display a Two-Step, Slow-Binding Inhibition Mechanism Which Is Absent in a Drug-Resistant T66I/M154I Mutant

Edward P. Garvey,*,‡ Benjamin Schwartz,§ Margaret J. Gartland,‡ Scott Lang,§ Wendy Halsey,|| Ganesh Sathe,|| H. Luke Carter III.,⊥ and Kurt L. Weaver⊥

Departments of Virology and Biological Reagents and Assay Development, GlaxoSmithKline Pharmaceuticals, 5 Moore Drive, Research Triangle Park, North Carolina 27709-3398, and Department of Biological Reagents and Assay Development and Discovery Technology Group, GlaxoSmithKline Pharmaceuticals, 1250 South Collegeville Road, Collegeville, Pennsylvania 19426-0989

Received November 19, 2008; Revised Manuscript Received December 31, 2008

ABSTRACT: Two-metal binding HIV-1 integrase inhibitors (INIs) are potent inhibitors of HIV-1 in vitro and in patients. We report here for the first time the kinetics of inhibition of integrase-catalyzed strand transfer. First, the IC_{50} values for each of six structurally distinct INIs decreased when a preincubation was included: S-1360 (1.3 μM vs 0.12 μM), L-731,988 (130 nM vs 9 nM), L-870,810 (130 nM vs 4 nM), raltegravir (300 nM vs 9 nM), elvitegravir (90 nM vs 6 nM), and GSK364735 (90 nM vs 6 nM). When reactions with these INIs were initiated with integrase, progress curve analyses indicated time-dependent inhibition, which could be fitted to a two-step mechanism of binding. Overall fitted K_i values matched the IC_{50} values measured with a preincubation: S-1360 (0.17 μM), L-731,988 (34 nM), L-870,810 (2.4 nM), raltegravir (10 nM), elvitegravir (4.0 nM), and GSK364735 (2.5 nM). To begin to understand the mechanism for this slow onset of inhibition and its possible impact on drug resistance, studies of resistance mutations were initiated. T66I/M154I exhibited little if any time-dependent inhibition by any of the six INIs, as measured by differences in potency upon preincubation or by progress curve analysis. These data demonstrate that slow binding is a signature of two-metal binding INIs, and that the second slow step is required for full potency. We discuss a possible structural explanation of the second slow step of inhibition and also the relationship between loss of time-dependent inhibition and drug resistance of this important new class of HIV-1 antiretroviral drugs.

Integrase, an essential enzyme in the retroviral life cycle, catalyzes two chemical reactions (3′ processing and strand transfer) that lead to the insertion of viral DNA into host DNA. The validation of integrase as an HIV[1] chemotherapeutic target has reached its highest level with the FDA approval of the first integrase inhibitor (INI), raltegravir (*1*). Over the past six years, at least five INIs have been tested in HIV-infected individuals: S-1360 (*2*), L-870,810 (*3*), raltegravir (*4*), elvitegravir (*5*), and GSK364735 (*6*). Four of these exploratory drugs have yielded 2-log or greater decreases in viral loads in phase IIa studies, reflecting a profound clinical effect in blocking this viral enzyme.

As impressive as the initial clinical data have been, it is already evident that INIs will present the same weakness as any antiretroviral, the emergence of resistant virus bearing mutation(s) within the target gene. Both in vitro passage studies (*3, 7*−*9*) and more importantly clinical data from phase II/III studies (*10*−*12*) have already highlighted key mutations that result in loss of in vitro potency and in clinical failure, respectively. We must understand the mechanism of resistance at the clinical, cellular, and especially molecular levels to best understand how to develop second-generation INIs that will overcome resistant mutations selected for by the initially approved drugs.

To best understand the molecular mechanisms of resistance, the mechanism and kinetics of inhibition should ideally first be well-described. Some of the key findings to date are as follows. (i) Potent INIs fall into the general scaffold of two-metal binders that bind the active site metals of integrase (*13*−*15*), presumably two magnesium ions (*16*). (ii) INIs selectively inhibit the second chemical reaction catalyzed by integrase (strand transfer) relative to the first reaction (3′-processing) (*16*−*18*). (iii) INIs potently bind only when integrase is in its binary complex with donor or viral DNA (*19*), possibly binding to a transient intermediate along the integration pathway (*20*). (iv) Terminal bases of the viral DNA play a role in both catalytic efficiency (*21, 22*) and inhibitor binding (*18, 23, 24*). (v) A mechanism of resistance

* To whom correspondence should be addressed. Phone: (919) 967-5972. E-mail: epgarvey@bellsouth.net.

‡ Department of Virology, GlaxoSmithKline Pharmaceuticals, Research Triangle Park, NC.

§ Department of Biological Reagents and Assay Development, GlaxoSmithKline Pharmaceuticals, Collegeville, PA.

|| Discovery Technology Group, GlaxoSmithKline Pharmaceuticals, Collegeville, PA.

⊥ Department of Biological Reagents and Assay Development, GlaxoSmithKline Pharmaceuticals, Research Triangle Park, NC.

[1] Abbreviations: HIV, human immunodeficiency virus; INI, integrase inhibitor; TDI, time-dependent inhibition; SPA, scintillation proximity assay; HEPES, 4-(2-hydroxyethyl)piperazine-1-ethanesulfonic acid; MOPS, 4-morpholinepropanesulfonic acid; EPPS, 3-[4-(2-hydroxyethyl)-1-piperazinyl]propanesulfonic acid; WT, wild type.

10.1021/bi802141y CCC: $40.75
Published on Web 01/29/2009

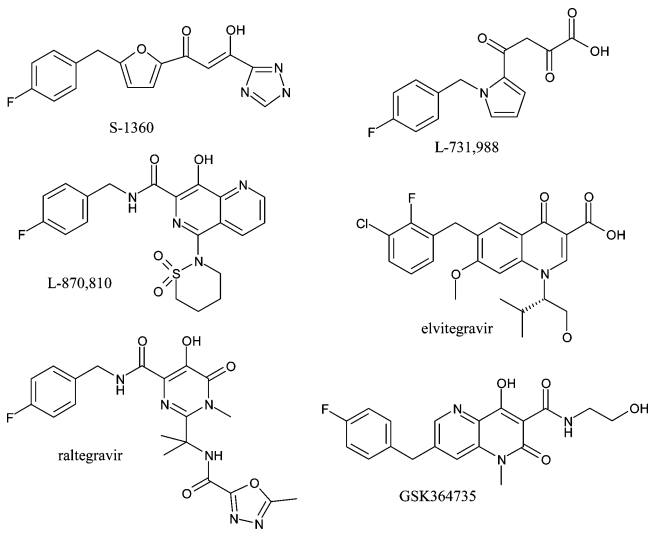

FIGURE 1: Chemical structures of INIs used in this study. Raltegravir has also been termed MK-0518 in the literature, and elvitegravir has been termed both JTK-303 and GS 9137.

for at least one particular INI is an increase in dissociation rate as measured in a binding assay (*25*). (vi) A flexible loop from residue 140 to 148 that plays a significant role in catalysis (*26*) has been implicated in inhibitor binding through molecular dynamic studies (*27*).

Some aspects of two-metal binding INI inhibition are not currently well defined, including the kinetics of inhibition. To the best of our knowledge, there has been no report to date that has examined the progress curves of strand transfer inhibition of this important new class of HIV chemotherapy. As has been highlighted in a recent review (*28*), it is critical to understand the kinetics of inhibition and in particular dissociation rates of potent drugs and drug candidates, as the residence time of an inhibitor on its target can considerably impact biological activity in vivo. Recent work has examined the kinetics of binding of one particular INI using a radiolabeled binding assay (*24, 25*) and has demonstrated that this INI is slow-binding. Using a scintillation proximity assay (SPA) that monitors the covalent insertion of target DNA into donor DNA, and a diverse collection of two-metal-binding scaffolds (Figure 1), we have complemented the finding described above by demonstrating that these inhibitors as a general class display a two-step, time-dependent inhibition (TDI) of integrase-catalyzed strand transfer. Furthermore, the drug-resistant double mutant T66I/M154I (*29*) did not display TDI, suggesting that these mutations alter the conformational sampling of integrase after initial inhibitor binding.

EXPERIMENTAL PROCEDURES

Reagents. Oligonucleotides used to make donor DNA were purchased from Invitrogen (Carlsbad, CA). Radiolabeled target DNA and streptavidin-coated scintillation proximity beads were purchased from GE Healthcare UK Limited (Buckinghamshire, U.K.).

Purification of HIV-1 Integrase. Full-length recombinant HIV-1 integrase was isolated from *Escherichia coli* BL21(DE3) carrying plasmid pT7-IN with the sequence of full-length HIV-1 integrase (*30*). Cells were thawed and lysed in buffer consisting of 50 mM Tris-HCl and 5 mM β-mercaptoethanol (pH 7.5) by being passed through an APV continuous-flow pressure cell at 10000 psi. After the lysate was centrifuged (SLA-1500 rotor, 14K rpm, 15 min), the pellet was resuspended in lysis buffer with a Polytron and centrifuged (SLA-1500 rotor, 10K rpm, 10 min). This wash was repeated on the resulting pellet. The twice-washed pellet was suspended in extraction buffer [50 mM Na-HEPES, 1 M $MgCl_2$, 50 μM $ZnCl_2$, and 1 mM β-ME (pH 7.0)] and left on ice for 1 h before centrifugation. All mutant integrase proteins were prepared by introducing the specific mutation into the wild-type sequence. These mutant proteins were expressed and purified using the same protocol as for the wild-type enzyme. Final protein concentrations ranged from 0.5 to 3 mg/mL, with purities ranging from 65 to 92%. In each preparation, background nuclease activity was tested for and not observed. DNA binding titrations of the wild-type preparation indicated that approximately 1% was capable of binding the donor DNA used in the strand transfer assay.

In Vitro Strand Transfer Assay. The strand transfer scintillation proximity assay (SPA) was previously described (*31*). Recombinant integrase was first bound to biotinylated unprocessed donor DNA oligonucleotide (attached to steptavidin beads). In separate reactions in which 3′-processing was assessed in a fluorescence polarization assay (using the unprocessed donor DNA with a fluorescein at the 3′-end) at 37 °C under the same conditions for the same length of time of the binary formation incubation, the fluorescence polarization signal decreased from 236 to 124 mP, an amount that represented 83% 3′-processing. Subsequent to binary complex formation and 3′-processing, strand transfer reactions were initiated. When the binary complex and inhibitor were preincubated, strand transfer was initiated with target DNA substrate. Reactions were quenched with a 3:1 volume addition of 25 mM MOPS (pH 6.5), 50 mM EDTA, 0.5 M NaCl, and 0.1% salmon sperm DNA. In this study, the standard assay buffer consisted of 25 mM Na-MOPS, 23 mM NaCl, and 10 mM $MgCl_2$ (pH 6.5). For pH optimum study, the following buffers were used: EPPS (pH 5.0−6.0), MOPS (pH 6.5−7.5), and HEPES (pH 7.5−9.0). The active wild-type integrase concentration was approximately 4 nM, and the target [^{3}H]DNA concentration was 6 nM. The E138K protein had 67% of the WT activity in the strand transfer assay and was used at the same relative amount as WT for all studies. The T66I/M154I double mutant had only 18% activity and was used at 4 times the amount of WT enzyme (the binary complex with donor DNA was formed under the same conditions as WT, taken up in $^1/_4$ of the final volume after the wash, and then used at the same dilution with the reaction mixture). All preincubations and single-time point determinations of IC_{50} values were as previously described (*31*). Time courses of inhibition were performed in 96-well plates which were thermostated at 37 °C. To minimize evaporation of the assay volume, a plate cover was used with a moist paper towel sandwiched between it and a prewarmed heat block on top of the cover, and the standard assay volume was increased to 30 μL, with all concentrations being the same. Individual wells were used for individual time points. For single-time point IC_{50} determinations, time courses were measured to determine the time point that produced maximal signal yet still was in a linear part of the reaction.

Sequence Analysis of Integrase-Catalyzed Strand Transfer SPA Products. To confirm that the observed SPA signal

correlated with covalent insertion of donor into target DNA, donor and target dsDNA oligos were synthesized with PCR primer sites (underlined). Note that the donor and target sequences for these substrates were repeated twice (total of three copies of the sequence) to allow for a more robust PCR signal. Biotinylated donor dsDNA was formed by annealing oligos 5′-biotin-GCA TGG CAG GAA AGA CCT ATG ACC ATG ATT ACC CTT TTA GTC AGT GTG GAA AAT CTC TAG ATT ACC CTT TTA GTC AGT GTG GAA AAT CTC TAG CA-3′ and 5′-ACT GCT AGA GAT TTT CCA CAC TGA CTA AAA GGG TAA TCT AGA GAT TTT CCA CAC TGA CTA AAA GGG TAA TCA TGG TCA TAG GTC TTT CCT G-3′. Unlabeled DNA and ^{3}H-labeled target dsDNA were made by annealing oligos 5′-GAC TCG AGA TTA TGG CGG TGA CCA AGG GCT AAT TCA TGA CCA AGG GCT AAT TCA TGA CCA AGG GCT AAT TCA C-3′ and 5′-AAA AAA AAG TGA ATT AGC CCT TGG TCA TGA ATT AGC CCT TGG TCA TGA ATT AGC CCT TGG TCA CCG CCA TAA TCT CGA GTC-3′ and filling in the 3′-end with either unlabeled dTTP or [^{3}H]dTTP with the Klenow fragment of DNA polymerase.

Reactions with ^{3}H-labeled target DNA were conducted as described above, at pH 6.5 in MOPS buffer. Similar SPA signals were observed with these reactions using the longer donor and target DNA oligos. Reactions using unlabeled target DNA were conducted under the same conditions but were subjected to PCR amplification and sequencing after quenching.

The two primers corresponding to viral DNA (CAGGAAAGACCTATGACCATGATT, primer A) and target DNA (GACTCGAGATTATGGCGG, primer B) were used to amplify the ligation products of the two DNA substrates. A control sample was also prepared; it contained only the two substrates, but no enzyme. The reaction mixtures for PCR contained 25 μL of *HotStarTaq Plus* Master Mix solution (Qiagen, Valencia, CA), each primer at 0.3 μM, and 5 ng of template DNA. An initial hot-start PCR step of 96 °C for 15 min was followed by 35 cycles of amplification (95 °C for 20 s, 55 °C for 30 s, and 72 °C for 45 s) and a final elongation step at 72 °C for 3 min. PCR products were subcloned into *pCR*2.1 vector (Invitrogen, Carlsbad, CA) and then transformed into competent *E. coli* by the TOPO TA cloning method (Invitrogen). Two hundred clones were picked for sequence analysis. The plasmid DNAs were purified from cultured bacteria with the QIAprep Spin Kit (Qiagen). DNA sequences of the cloned inserts were determined using vector-specific sequencing primers. PCR products were not detected for the control reaction. Sequencing of plasmid DNA was performed with the BigDye Terminator cycle sequencing kit and a Genetic Analyzer 3100 (both from Applied Biosystems, Foster City, CA). The sequences were compiled and analyzed with Sequencher (Gene Codes Corp, Ann Arbor, MI).

PBMC HIV Replication Cell Assay. HIV-1 Ba-L replication in PBMCs in a 7 day assay was quantitated by measuring reverse transcriptase activity present in the supernatant, as previously described (*6*).

Fitting of Enzyme Inhibition Data. Titration data were fit to the equation $y = V_{max}I/(IC_{50} + I)$, where y is the normalized signal and I is the concentration of inhibitor, to determine the apparent IC_{50} value for the inhibitor. Fitting of the progress curves was based on the methods developed by Morrison and Walsh (*32*) for a two-step model of inhibition:

$$E + I \rightleftharpoons EI \rightleftharpoons EI^*$$

where enzyme (E) and inhibitor (I) form an initial complex (EI), which then isomerizes to a tighter complex (EI*). The progress curve for each inhibitor concentration was fit (using Grafit) to eq 1:

$$P = V_s t + (V_o - V_s)(1 - e^{-kt})/k + C \quad (1)$$

where P is the signal from product, V_s is the final, steady-state velocity, V_o is the initial velocity, k is the rate constant associated with the transition from the initial to final velocity, and C is the background signal at time zero. The rate constant (k) and associated error were then plotted against the concentration of inhibitor according to eq 2 to produce the values for K_i, k_5, and k_6 (nomenclature from ref *32*):

$$k = k_6 + k_5[I/K_{i,initial}/(1 + A/K_a + I/K_{i,initial})] \quad (2)$$

where $K_{i,initial}$ is the inhibition constant for the initial EI complex, A is equal to the substrate concentration, K_a is the Michaelis constant for substrate A, and k_5 and k_6 represent the individual rate constants for the forward and reverse steps of the EI ↔ EI* transition, respectively. In the course of this work, the concentration of A (target DNA) was fixed at $\ll K_a$. The values of V_s obtained from the fits of the progress curves were also plotted versus the concentration of inhibitor according to eq 3 to yield $K_{i,final}$, the overall inhibition constant:

$$V_s = VA/[K_a(1 + I/K_{i,final}) + A] + B \quad (3)$$

where V represents the velocity in the absence of inhibitor, B represents the background (no integrase) rate, and the other variables are as described above.

RESULTS

Characterization of HIV Integrase Strand Transfer SPA. The binary complex of purified HIV integrase and biotinylated donor DNA (which was bound to streptavidin beads) was used to initiate the strand transfer reaction with radiolabeled target DNA. For simplification of terminology, the binary complex of integrase and donor DNA will be subsequently termed integrase. It is noted that the oligonucleotide DNA corresponding to the HIV-1 U5 LTR DNA is termed donor DNA, while the DNA corresponding to the random host DNA is termed target DNA. The increase in the magnitude of the signal (i.e., enhanced chemiluminescence) resulted from the proximity of covalently attached radiolabeled DNA to the SPA bead. This increase in signal was time-, enzyme-, and metal ion-dependent (data not shown). The target DNA showed saturation kinetics with a K_m value of 50 ± 5 nM (Figure 2A). The pH optimum was 6.5 for both V_{max} versus pH (Figure 2B) and V/K_m versus pH (data not shown). Finally, to definitively demonstrate that the observed SPA signal was due to integrase-catalyzed insertion of donor into target, a nonradiolabeled version of the reaction was conducted, and the products were amplified by PCR using primers from both the donor and target substrates. Without enzyme added, no products were amplified. However, with integrase, 23 different insertion products

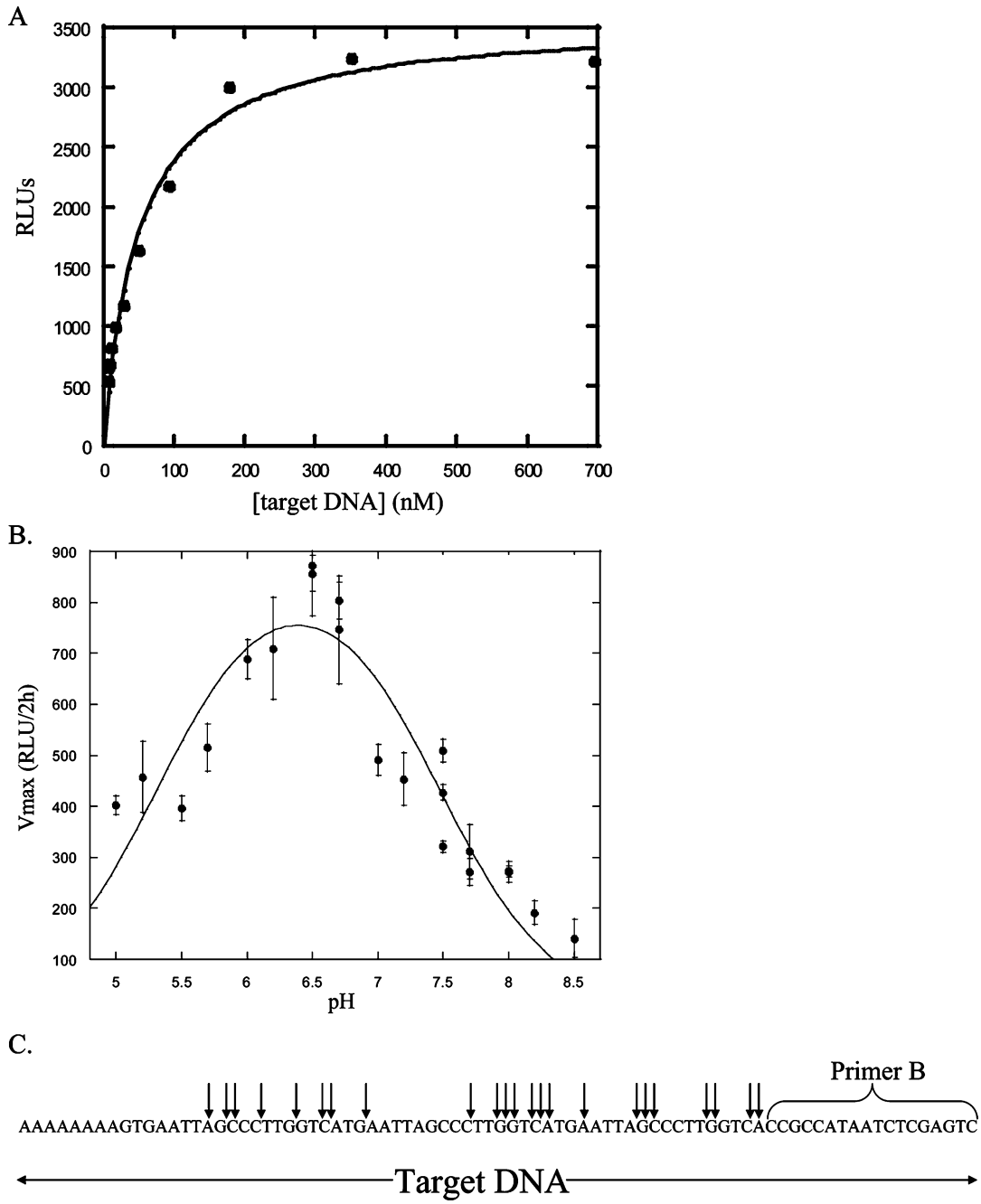

FIGURE 2: Characterization of strand transfer SPA. Strand transfer SPA is described in Experimental Procedures. RLU on *y*-axis is defined as relative light unit. (A) Target substrate [^{3}H]DNA displayed saturation kinetics. The target [^{3}H]DNA concentration was varied between 2.5 and 700 nM; initial rates were determined, and the Michaelis−Menten equation was fitted to data. (B) The pH optimum of SPA was 6.5. Buffers and pH ranges are described in Experimental Procedures. (C) Arrows indicate where donor DNA inserted into target DNA, as determined by sequencing of strand transfer SPA products.

were identified, dispersed throughout the target DNA (Figure 2C). This characterization confirmed that the assay monitored the covalent insertion of donor into target DNA and that the SPA was a viable approach for studying the kinetics of HIV integrase.

Preincubation Studies of TDI of Recombinant Integrase. The inhibition potencies of six INIs (Figure 1) were first determined in assays which were initiated with the integrase at a single time point of 10 min. These potencies were all relatively weaker than antiviral potencies that were measured in a multiday replication assay (Table 1). One potential explanation for such a discrepancy is time-dependent inhibition, where the potency of the inhibitor increases over time. This possibility was tested at the enzyme level by including a preincubation of INI with integrase for 60 min at 37 °C. The six inhibitors showed an 11−33-fold increase in potency, with the average increase being 20-fold (Table 1). The potencies with preincubation were much closer to the antiviral potencies measured in cells (except for that of L-731,988), suggesting that these values were more relevant and that there was a slow step in the inhibition of integrase.

The data presented above were generated with a binary complex formed between integrase and unprocessed donor DNA substrate followed by 3′-processing prior to initiation of the strand transfer reaction (see Experimental Procedures). When the binary complex was formed with a fully processed donor DNA (i.e., the two 3′-terminal nucleotides absent in the synthesized oligo), potencies with and without preincu-

Table 1: Biochemical Potencies of INIs in the Strand Transfer SPA with and without Preincubation, Relative to Antiviral Potencies[a]

	SPA (blunt-end donor[b]) IC_{50} (nM)			SPA (processed donor[b]) IC_{50} (nM)			
	no preincubation	preincubation	TDI ratio	no preincubation	preincubation	TDI ratio	antiviral EC_{50} (nM) for the 7 day replication
S-1360	1300 (100)	120 (40)	11	1800 (100)	200 (30)	9	820 (200)
L-731,988	130 (60)	9 (4)	14	160 (20)	20 (5)	8	3900 (600)
L-870,810	130 (50)	4 (2)	32	190 (30)	8 (3)	24	3 (1)
elvitegravir	90 (20)	6 (3)	15	110 (40)	6 (2)	18	2.1 (0.7)
raltegravir	300 (100)	9 (4)	33	250 (50)	9 (3)	28	2.4 (0.6)
GSK364735	90 (40)	6 (3)	15	130 (40)	7 (3)	18	1.9 (0.5)

[a] Values are average (standard deviation) of multiple determinations, using recombinant integrase in a strand transfer SPA ($N > 3$) and antiviral assay ($N > 3$) as described in Experimental Procedures. [b] Indicates which donor DNA substrate was used to form the integrase−donor DNA complex.

bation were the same within experimental error (Table 1). These data demonstrate that the slow onset of inhibition does not require the catalytic event of 3′-processing to activate a particular conformation of enzyme.

Kinetic Studies of TDI of Integrase. To characterize the slow onset of inhibition in kinetic studies, strand transfer reactions with INIs were initiated with enzyme and quenched at multiple time points. Figure 3A shows progress curves of the reaction with varying L-870,810 concentrations. Compared to the uninhibited control, progress curves with L-870,810 display classic time-dependent behavior, with increasing inhibition observed as greater reaction times. Figure 3B shows a replot of the observed first-order rate constant (corresponding to the onset of the slow phase of inhibition) versus inhibitor concentration, which displayed saturation kinetics. From this replot, initial K_i, k_5, and k_6 values could be determined (Table 2) for the classical two-step binding mechanism described by Morrison and Walsh (*32*):

$$E + I \overset{K_{i,initial}}{\rightleftharpoons} EI \underset{k_6}{\overset{k_5}{\rightleftharpoons}} EI^*$$

In addition, the steady-state inhibited rate was plotted versus inhibitor concentration (Figure 3C) to yield the steady-state or final K_i for inhibitor. Note that the effect of inhibitor on the steady-state rate reached a maximal effect and a minor rate of approximately 3% of the control rate remained. For these analyses, this rate was deemed a background rate.

These experiments were repeated for each of the other INIs. For each inhibitor, the same slow onset of inhibition was observed in the progress curves (data not shown). Table 2 displays the initial and final K_i values and the on and off rates for each of the inhibitors. As would be expected from this model, the final K_i values (Table 2) matched closely the IC_{50} values determined when preincubation was included (Table 1).

These kinetic data were generated using the binary complex that was formed with integrase and unprocessed donor DNA followed by 3′-processing, prior to initiation of the particular kinetic study. We observed the same slow-binding kinetics with these INIs when the binary complex was made with integrase and fully processed donor DNA. For example, when S1360 was used as an INI, the rate constants ($k_5 = 0.39$ min^{-1}, and $k_6 = 0.032$ min^{-1}) and K_i values ($K_{i,initial} = 2050$ nM, and $K_{i,final} = 290$ nM) were 1.2- to <3.1-fold of the values in Table 2. Therefore, as mentioned above, the time-dependent inhibition was not dependent on a particular conformation of integrase induced by its catalysis of 3′-processing.

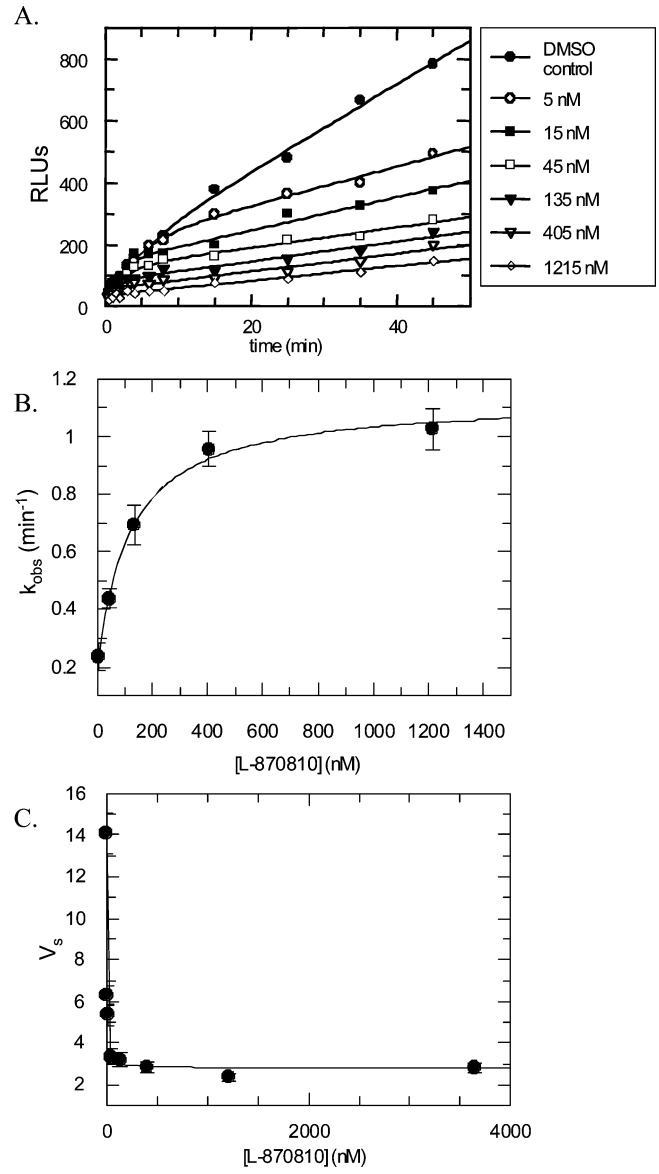

FIGURE 3: Slow onset of strand transfer inhibition of wild-type integrase by L-870,810. (A) Progress curves in which the L-870,810 concentration was varied as indicated compared to the control reaction without inhibitor. Reactions described in Experimental Procedures with the indicated inhibitor concentrations, 6 nM target [^{3}H]DNA, and initiated with wild-type integrase at 37 °C. Equation 1 was fitted to each progress curve. (B) Replot of data in which the first-order rate constant determined from the progress curve was plotted vs L-870,810 concentration. (C) Replot of data in which the steady-state velocity determined from the progress curve was plotted vs L-870,810 concentration.

Effects of Mutations on TDI of Integrase. In an attempt to understand the structural basis for the slow onset of inhibi-

Table 2: Kinetic Parameters for Slow Onset Inhibition of HIV Integrase

	$K_{i,initial}$ (nM)	$K_{i,final}$ (nM)	k_5 (min^{-1}) (k_{on})	k_6 (min^{-1}) (k_{off})
S1360	1700 (1300)	170 (30)	0.83 (0.15)	<0.1
L-731,988	222 (76)	34 (13)	0.65 (0.05)	0.11 (0.04)
L-870,810	115 (23)	2.4 (0.5)	0.94 (0.05)	0.19 (0.04)
elvitegravir	230 (150)	4 (1)	1.1 (0.2)	0.5 (0.1)
raltegravir	200 (100)	10 (3)	1.0 (0.1)	0.15 (0.09)
GSK364735	280 (440)	2.5 (0.4)	1.0 (0.4)	0.3 (0.1)

[a] Values (standard error) are from fits of equations to progress curve data from the strand transfer SPA as described in Experimental Procedures.

tion, we have begun to examine resistance mutations. First, as a control for the lack of effect on TDI, we tested E138K, which had little effect on inhibitor binding and on integrase activity. This mutation has been observed as a secondary mutation linked to mutations at Q148 (*9, 33*). The relative lack of an effect at the viral replication level (*33, 34*) was confirmed at the purified protein level as the E138K recombinant protein had 67% of WT integrase strand transfer activity. When E138K was used in titrations and kinetic studies, TDI was observed. Each of the six INIs was more potent with preincubation included (Table 3), and curvature relative to control was observed when two INIs, L-870,810 and S1360, were examined kinetically (data not shown). For five of the six INIs, the TDI ratios for the E138K enzyme were similar or the same as the wild-type ratios, and there was a minimal effect on potency of inhibition (i.e., little or no resistance). However, for L-731,988, the TDI ratio decreased 7-fold (from 14- to 2-fold), which closely matched the 6-fold decrease in potency observed with this mutation. This suggested that for this INI and mutation, resistance may be due to the partial loss of time-dependent inhibition.

The T66I/M154I resistance double mutant was identified from a passage study with L-731,988 (*29*). It was chosen on the basis of a molecular dynamics simulation study (*27*), which suggested these mutations concomitantly affected the conformation of the flexible loop from residue 140 to 148 and the binding of an early two-metal binder 5-ClTEP. As in a recent report (*35*), this double mutation significantly decreased activity (18% of that of WT integrase). When inhibitors were titrated with and without preincubation, two findings were notable (Table 3). First, effects on potency comparing wild-type to mutant integrase were observed that were consistent with fold resistance values in the literature for the double mutant itself (or using T66I as a comparator mutant virus). Second, and of greater interest, very small if any changes were observed in compound potencies with preincubation. The largest increase in potency was a 3-fold increase observed with raltagravir; all other increases were ≤2-fold. None of the statistical comparisons between IC_{50} values determined with and without preincubation were significantly different [*p* values ranging from 0.09 to 0.43 (Table 3)]. Furthermore, when progress curves were collected using L-870,810 (Figure 4A), raltegravir, or L-731,988 (data not shown), no evidence of curvature relative to control was observed. The K_i value calculated from the linear rate versus L-870,810 concentration relationship (Figure 4B) was 21 ± 8 nM, which was the same as the IC_{50} value with preincubation derived from a single-time point titration (Table 3). Thus, there was no evidence of TDI with T66I/M154I integrase.

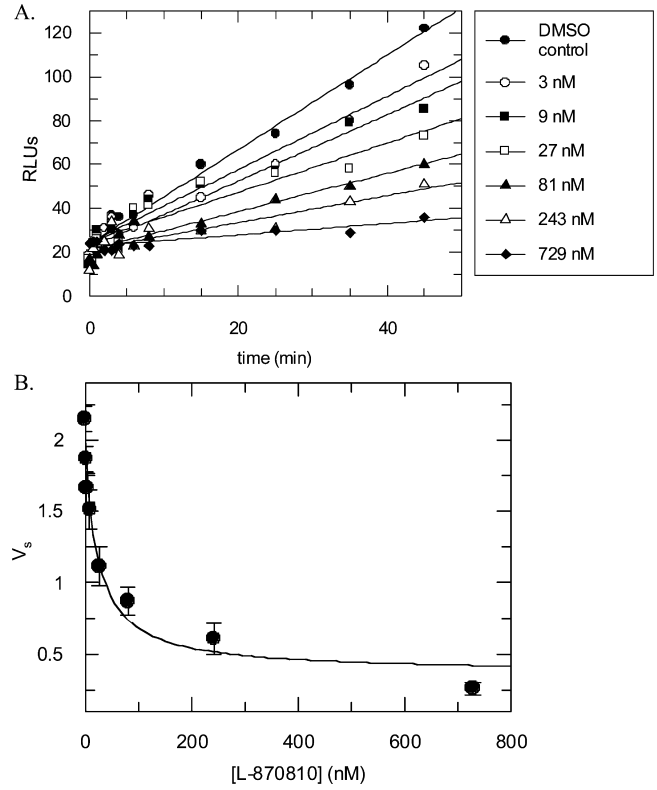

FIGURE 4: L-870,810 inhibition of T66I/M154I integrase is not time-dependent. (A) Progress curves in which the L-870,810 concentration was increased as indicated compared to the control reaction without inhibitor. Reactions are described in Experimental Procedures with the indicated inhibition concentrations, 6 nM target [^{3}H]DNA, and initiation with T66I/M154I integrase at 37 °C. Equation 1 did not successfully fit any progress curve, whereas a linear equation did fit. (B) Replot of data in which linear velocity was plotted vs L-870,810 concentration.

DISCUSSION

The potent inhibitors of HIV integrase that bind to the binary complex of enzyme and viral DNA all exhibited a slow onset of inhibition that could be modeled by a two-step process. Whereas the potencies of these molecules have been described at the level of half-maximal inhibitory concentrations (IC_{50} values) in cellular antiviral and recombinant enzyme assays, kinetic analyses and slow-binding inhibition of integrase-catalyzed strand transfer by two-metal binding inhibitors are novel disclosures. This relatively slow process was observed in preincubation and in kinetic studies, and the overall potency as determined by both methods was approximately the same. Furthermore, strand transfer studies with preintegration complexes isolated from virally infected cells also demonstrated that these inhibitors are more potent if a preincubation step is included (M. Xie, M. R. Underwood, and E. P. Garvey, unpublished data). Additionally, a recent report (*24*) described two-step slow-binding kinetics for the binding of one particular INI to the integrase−donor DNA binary complex. Models for two-step kinetics have been described by Morrison and Walsh (*32*) and propose that the inhibitor binds the target in an initial complex, followed by a slow step to a tighter complex that occurs on a relatively slow time scale (often minutes to hours). This slow inhibition by INIs was not a function of their overall potency as the same kinetics were observed with the five low nanomolar inhibitors as with S1360 which is ap-

proximately 100 times weaker. Thus, this two-step, slow-binding inhibition appears to be a signature of two-metal binding INIs.

Copeland and colleagues (*28*) recently reviewed drugs or drug candidates that display a slow onset of inhibition and, in particular, focused on the slow dissociation of such molecules from their molecular targets. They emphasized that slow dissociation or long residence times of inhibitor bound to target potentially lead to prolonged pharmacological effects in vivo. It is not known at this time if the dissociation rates measured in these kinetic studies specifically contribute to the highly significant efficacy demonstrated with INIs in clinical studies. However, it is clear that this class of antiretroviral does show one of the highest levels of viral load suppression in HIV-infected patients, and that the overall slow-binding second step described in this study increased potency on average approximately 20-fold.

Slow inhibition that fits the two-step model sometimes results from a conformational change that leads to tighter interaction(s). Given the proposed binding of INIs to the active site metal ions of integrase and the hypothesis that the flexible loop from residue 140 to 148 plays a role in catalysis and inhibitor binding (*26, 27*), this slow step may reflect a rearrangement of this stretch of peptide that strengthens interactions of enzyme and inhibitor. For many enzymes, slow inhibition kinetics have been postulated or proven to be caused by movement of flexible loops or flaps (*36*−*39*). Furthermore, several resistance mutations to integrase inhibitors are located at the ends of this loop, and these mutations may selectively affect the rate constants for the slow step compared to the initial binding constant. In addition, mutations distant from the loop in primary sequence may also affect the movement of the loop. A molecular dynamics simulation (*27*) suggested that the double mutation T66I/M154I may have such effects, increasing the flexibility of the 140−148 loop and also yielding different binding modes for a two-metal binding inhibitor.

We therefore tested whether the various INIs exhibited time-dependent inhibition of T66I/M154I. First, the INIs displayed the expected loss of potency against this mutation which was derived from resistance passage studies. For example, L-731,988, which was used in passage studies that isolated this double mutant (*29*), had an 11-fold decrease in potency compared to that of the wild-type enzyme; this compares well with the published 15-fold decrease in potency (*29*). Second, of greater interest, there was no TDI with any of the INIs in either preincubation or kinetic studies. Thus, these two mutations have eliminated the slow step in inhibition by these two-metal binders. Coupled with the observations cited above, a working hypothesis can be made to guide future experiments. INI binds to the active site magnesium ions of integrase in an initial complex that has a binding K_i in the low hundreds in nanomolar. For wild-type integrase, this binding triggers a conformational change in the neighboring 140−148 loop that leads to additional interaction(s) and a final K_i in the low single-digit nanomolar range. For T66I/M154I, this conformational change either does not occur or occurs incompletely.

An alternative molecular model for the slow step in INI binding or inhibition has been proposed on the basis of the effects that changes to the terminal 3′-adenosine of the processed donor DNA have on the kinetics of binding of one particular INI (*24*). The composite on rate (of a two-step model) increased with changes to the terminal adenosine (for example, removal of parts of the adenosine or changes to the base). The authors hypothesized that the terminal adenosine may exist in two conformations ("open" and "closed") and that the interconversion between these dictates the kinetics of INI binding. Although the kinetics described in the binding assay (*24*) are similar to the kinetics reported here, there are differences. One difference is that whereas a two-step model best fit the binding data collected at 20 °C, a single-step model fitted the binding data measured at 37 °C, which could be attributed to the second step becoming too fast to measure at the higher temperature (*24*). This is in contrast to our study that was conducted at 37 °C and where the data were best fit to the two-step inhibition model. Thus, whereas it is tempting to view these two descriptions of INI slow-binding kinetics as measuring the same molecular events, it is possible that they are different, and hence, the molecular mechanism could be different. If they are measuring the same events, it is formally possible that the two hypotheses are both correct: The T66I and M154I mutations may alter the conformation of the terminal adenosine through effects on the conformation of the loop. Obviously, further experiments are required to develop and differentiate these hypotheses.

Is the elimination of TDI the mechanism of resistance for this particular double mutant? For three of the INIs, it does appear to be the molecular mechanism. The fold resistances for S1360, L-731,988, and elvitegravir closely match the potency gained by TDI (as measured by the ratio of IC_{50} values with and without preincubation). However, for the other three INIs (raltegravir, GSK364735, and L-870,810), even though TDI is absent, overall potency was retained, as the mutations also affected the initial potency of binding. These two groups of INIs may reflect different chemical scaffolds, insofar as both S1360 and L-731,988 are diketo acid-like and both GSK364735 and L-870,810 are naphthyridine-like. Thus, at least with this particular resistance mutant, there is a complicated interplay among scaffold, resistance, and TDI.

As mentioned, this slow onset of inhibition is a novel finding, and one can ask how these data correlate with previous descriptions of potency determined at single time points. L-870,810 represents the most complete literature description of inhibition of the compounds used in this study (*3*). Its inhibition of the strand transfer reaction measured at a single time point of 30 min had an IC_{50} value of 15 nM when 5 nM target DNA was used (*3*). The stated conditions of the assay were that inhibitor was added to binary complex and then target DNA was "added immediately". Therefore, this approximates a reaction initiated by enzyme. When the 30 min point in the curves shown in Figure 3A are plotted against L-870,810 concentration, the approximate IC_{50} is 20 nM (in near agreement with the 15 nM value). Furthermore, in the same reference, in a binding assay using a radiolabeled INI that presumably allows an inhibitor time to reach equilibrium with the binary complex, L-870,810 had a K_i value of 3 nM. This is essentially the same as the $K_{i,final}$ value of 2.3 nM in this study using the analyses of time courses. Finally, in a reference from a different laboratory (*40*), the state potency of L-870,810 was 1 nM when it was first preincubated with the binary complex for 30 min at room

Table 3: Comparison of INI Potencies (with or without preincubation) against Wild-Type and Mutant Integrases[a]

	wild-type IC_{50} (nM)				E138K IC_{50} (nM)						T66I/M154I IC_{50} (nM)					
	no preincubation	preincubation	p value[b]	TDI ratio[c]	no preincubation	preincubation	p value	TDI ratio	FR[d] vs WT	FR p value[e]	no preincubation	preincubation	p value	TDI ratio	FR vs WT	FR p value
S-1360	1300 (100)	120 (40)	3×10^{-5}	11	3100 (1800)	174 (47)	3×10^{-3}	21	1	0.10	1600 (500)	1600 (700)	0.43	1	13	2×10^{-3}
L-731,988	130 (60)	9 (4)	5×10^{-4}	14	116 (51)	58 (17)	2×10^{-2}	2	6	2×10^{-3}	100 (40)	100 (90)	0.39	1	11	6×10^{-4}
L-870,810	130 (50)	4 (2)	1×10^{-4}	32	129 (69)	13 (4)	5×10^{-3}	10	3	6×10^{-4}	90 (20)	50 (30)	0.11	2	8	0.01
elvitegravir	90 (20)	6 (3)	1×10^{-5}	15	97 (25)	8 (3)	5×10^{-5}	12	1	0.09	20 (10)	10 (5)	0.12	2	2	0.04
raltegravir	300 (100)	9 (4)	2×10^{-4}	33	151 (60)	12 (4)	8×10^{-4}	12	1	0.47	70 (80)	20 (10)	0.39	3	2	0.07
GSK364735	90 (40)	6 (3)	1×10^{-3}	15	118 (40)	13 (4)	4×10^{-4}	9	2	0.01	15 (9)	7 (4)	0.09	2	1	0.27

[a] Values are the average (standard deviation) of multiple determinations ($N > 3$), using recombinant integrase as described in Experimental Procedures. [b] t test analysis of whether the two IC_{50} values (with or without preincubation) are statistically different. [c] Time-dependent inhibition ratio = IC_{50}(without preincubation)/IC_{50}(with preincubation). [d] Fold resistance vs the wild type comparing potencies with preincubation included. [e] t test analysis to determine if FR vs the wild type is statistically different.

temperature, after which inhibition was assessed at a single time point of 90 min at room temperature.

The two-step model used to describe the slow onset predicts that $K_{i,final} = K_{i,initial}[k_6/(k_6 + k_5)]$. This relationship is observed with the kinetic analyses for S1360, L-731,988, and raltegravir (the $K_{i,final}$ derived from this relationship was within a factor of 3 of the value derived from the V_s versus [I] replot). However, L-870,810, elvitegravir, and GSK364735 showed 8-, 18-, and 26-fold differences, respectively. Because the $K_{i,final}$ values derived from the replots of V_s versus [I] match the IC_{50} values measured after preincubation (and the antiviral potencies measured in cells), these values are likely to be more accurate. It is possible that these differences might in part be due to the active enzyme concentration being similar to the K_i values, especially for the more potent INIs (note that the largest differences were observed for the more potent inhibitors). Alternatively, the calculated $K_{i,final}$ values may be affected by the observation of slight nonlinearity in the control progress curves prior to the linear steady-state rate. We do not know the cause of this behavior at present. For inhibitors with slow off rates, it will be difficult to measure k_6 experimentally, because the onset of time-dependent inhibition at low inhibitor concentrations (where k_6 predominates) may be so slow that it approaches the behavior observed in the controls. As a result of this, the k_6 values we have listed in Table 2 should be considered upper estimates, and the $K_{i,final}$ values calculated from them may be higher than the true values (as was observed for L-870,810, elvitegravir, and GSK364735).

Further studies of other recombinant mutant integrase enzymes and other INI scaffolds are underway to test these hypotheses of linking TDI with the flexible 140−148 loop and linking TDI with resistance. Regardless of the specific outcomes of these additional studies, the observation of a slow step in INI kinetics provides another parameter to measure when the effects of resistance mutations are examined. These parameters may add to our understanding of the molecular mechanism of both inhibition and resistance of this important new class of medicine for treating HIV infection.

ACKNOWLEDGMENT

We thank Brian Johns for exemplary leadership of the medicinal chemistry effort which led to the discovery and development of GSK364735, Sara Thrall and Gary Smith for discussion of the manuscript, Rob Ferris for testing the inhibitors in the PBMC antiviral assay, and the entire Shionogi-GSK integrase research team for providing a foundation of scientific excellence in the field of integrase drug discovery.

REFERENCES

1. Croxtall, J. D., Lyseng-Williamson, K. A., and Perry, C. M. (2008) Raltegravir. *Drugs 68*, 131–138.
2. Billich, A. (2003) S-1360 Shionogi-GlaxoSmithKline. *Curr. Opin. Invest. Drugs 4*, 206–209.
3. Hazuda, D. J., Anthony, N. J., Gomez, R. P., Jolly, S. M., Wai, J. S., Zhuany, L., Fisher, T. E., Embrey, M., Guare, J. P., Egbertson, M. S., Vacca, J. P., Huff, J. R., Felock, P. J., Witmer, M. V., Stillmock, K. A., Danovich, R., Gobler, J., Miller, M. D., Espeseth, A. S., Jin, L., Chen, I.-W., Kassahun, K., Ellis, J. D., Wong, B. K., Xu, W., Pearson, P. G., Schleif, W. A., Cortese, R., Emini, E., Summa, V., Holloway, M. K., and Young, S. D. (2004) A

naphthyridine carboxamide provides evidence for discordant resistance between mechanistically identical inhibitors of HIV-1 integrase. *Proc. Natl. Acad. Sci. U.S.A. 101*, 11233–11238.
4. Markowitz, M., Morales-Ramirez, J. O., Nguyen, B.-Y., Kovacs, C. M., Steigbigel, R. T., Cooper, D. A., Liporace, R., Schwartz, R., Isaacs, R., Gilde, L. R., Wenning, L., Zhao, J., and Teppler, H. (2006) Antiretroviral activity, pharmacokinetics, and tolerability of MK-0518, a novel inhibitor of HIV-1 integrase, dosed as monotherapy for 10 days in treatment-naive HIV-1-infected individuals. *J. Acquired Immune Defic. Syndr. 43*, 509–515.
5. DeJesus, E., Berger, D., Markowitz, M., Cohen, C., Hawkins, T., Ruane, P., Elion, R., Farthing, C., Zhong, L., Cheng, A. K., McColl, D., and Kearney, B. P. (2006) Antiviral activity, pharmacokinetics, and dose response of the HIV-1 integrase inhibitor GS-9137 (JTK-303) in treatment-naive and treatment-experienced patients. *J. Acquired Immune Defic. Syndr. 43*, 1–5.
6. Garvey, E. P., Johns, B. A., Gartland, M. J., Foster, S. A., Miller, W. H., Ferris, R. G., Hazen, R. J., Underwood, M. R., Boros, E. E., Thompson, J. B., Weatherhead, J. G., Koble, C. S., Allen, S. H., Schaller, L. T., Sherrill, R. G., Yoshinaga, T., Kobayoshi, M., Wakasa-Morimoto, C., Miki, S., Nakahara, K., Noshi, T., Sato, A., and Fujiwara, T. (2008) The naphthyridinone GSK364735 is a novel, potent human immunodeficiency virus-1 integrase inhibitor and antiretroviral. *Antimicrob. Agents Chemother. 52*, 901–908.
7. Shimura, K., Kodama, E., Sakagami, Y., Matsuzaki, Y., Watanabe, W., Yamataka, K., Watanabe, Y., Ohata, Y., Doi, S., Sato, M., Kano, M., Ikeda, S., and Matsuoka, M. (2008) Broad antiretroviral activity and resistance profile of the novel human immunodeficiency virus integrase inhibitor elvitegravir (JTK-303/GS-9137). *J. Virol. 82*, 764–774.
8. Hombrouck, A., Voet, A., Van Remoortel, B., Desadeleer, C., De Maeyer, M., Debyser, Z., and Witvrouw, M. (2008) Mutations in human immunodeficiency virus type 1 integrase confer resistance to the naphthyridine L-870,810 and cross-resistance to the clinical trial drug GS-9137. *Antimicrob. Agents Chemother. 52*, 2069–2078.
9. Kobayashi, M., Nakahara, K., Seki, T., Miki, S., Kawauchi, S., Suyama, A., Wakasa-Morimoto, C., Kodama, M., Endoh, T., Oosugi, E., Matsushita, Y., Murai, H., Fujishita, T., Yoshinaga, T., Garvey, E., Foster, S., Underwood, M., Johns, B., Sato, A., and Fujiwara, T. (2008) Selection of diverse and clinically relevant integrase inhibitor-resistant human immunodeciency virus type 1 mutants. *Antiviral Res.* (in press).
10. Hazuda, D. J., Miller, M. D., Nguyen, B. Y., and Zhao, J. (2007) Resistance to the HIV-integtrase inhibitor raltegravir: Analysis of protocol 005, a phase 2 study in patients with triple-class resistant HIV-1 infection. XVI International Drug Resistance Workshop, Antiviral Therapy, Bridgetown, Barbados, June 12−16, 2007; 12: S10.
11. McColl, D. J., Fransen, S., Gupta, S., Parkin, N., Margot, N., Ledford, R., Chen, J., Chuck, S., Cheng, K., and Miller, M. D. (2007) Resistance and cross-resistance to first generation integrase inhibitors: Insights from a phase 2 study of elvitegravir (GS-9137). XVI International Drug Resistance Workshop, Antiviral Therapy, Bridgetown, Barbados, June 12−16, 2007; 12:S11.
12. Malet, I., Delelis, O., Valantin, M.-A., Montes, B., Soulie, C., Wirden, M., Tchertanov, L., Peytavin, G., Reyenes, J., Mouscadet, J.-F., Katlama, C., Calvez, V., and Marcelin, A.-G. (2008) Mutations associated with failure of raltegravir treatment affect integrase sensitivity to the inhibitor in vitro. *Antimicrob. Agents Chemother. 52*, 1351–1358.
13. Barreca, M. L., Ferro, S., Rao, A., DeLuca, L., Zappala, M., Monforte, A.-M., Debyser, Z., Witvrouw, M., and Chimirri, A. (2005) Pharmacophore-based design of HIV-1 integrase strand-transfer inhibitors. *J. Med. Chem. 48*, 7084–7088.
14. Kawasuji, T., Fuji, M., Yoshinaga, T., Sato, A., Fujiwara, T., and Kiyama, R. (2006) A platform for designing HIV integrase inhibitors. Part 2: A two-metal binding model as a potential mechanism of HIV integrase inhibitors. *Bioorg. Med. Chem. 14*, 8420–8429.
15. Dayam, R., Al-Mawsawi, L. Q., Zawahir, Z., Witvrouw, M., Debyser, Z., and Neamati, N. (2008) Quinolone 3-carboxylic acid pharmacophore: Design of second generation HIV-1 integrase inhibitors. *J. Med. Chem. 51*, 1136–1144.
16. Grobler, J. A., Stillmock, K., Hu, B., Witmer, M., Fetlock, P., Espeseth, A. S., Wolfe, A., Egbertson, M., Bourgeois, M., Melamed, J., Wai, J. S., Young, S., Vacca, J., and Hazuda, D. J. (2002) Diketo acid inhibitor mechanism and HIV-1 integrase: Implications for metal binding in the active site of phosphotransferase enzymes. *Proc. Natl. Acad. Sci. U.S.A. 99*, 6661–6666.
17. Marchand, C., Zhang, X., Pais, G. C. G., Cowansage, K., Neamati, N., Burke, T. R., Jr., and Pommier, Y. (2002) Structural determinants for HIV-1 integrase inhibition by β-diketo acids. *J. Biol. Chem. 277*, 12596–12603.
18. Johnson, A. A., Marchand, C., Patil, S. S., Costi, R., DiSanto, R., Burke, R. R., Jr., and Pommier, Y. (2007) Probing HIV-1 integrase inhibitor binding sites with position-specific integrase-DNA cross-linking assays. *Mol. Pharmacol. 71*, 893–901.
19. Espeseth, A. S., Felock, P., Wolfe, A., Witmer, M., Grobler, J., Anthony, N., Egbertson, M., Melamed, J. Y., Young, S., Hamill, T., Cole, J. L., and Hazuda, D. J. (2000) HIV-1 integrase inhibitors that compete with the target DNA substrate define a unique strand transfer conformation for integrase. *Proc. Natl. Acad. Sci. U.S.A. 97*, 11244–11249.
20. Pandey, K. K., Bera, S., Zahm, J., Vora, A., Stillmock, K., Hazuda, D., and Grandgenett, D. P. (2007) Inhibition of human immunodeficiency virus type 1 concerted integration by strand transfer inhibitors which recognize a transient structural intermediate. *J. Virol. 81*, 12189–12199.
21. Sherman, P. A., Dickson, M. L., and Fyfe, J. A. (1992) Human immunodeficiency virus type 1 integration protein: DNA sequence requirements for cleaving and joining reactions. *J. Virol. 66*, 3593–3601.
22. Johnson, A. A., Santos, W., Pais, G. C. G., Marchand, C., Amin, R., Burker, T. R., Jr., Verdine, G., and Pommier, Y. (2006) Integration requires a specific interaction of the donor DNA terminal 5′-cytosine with glutamine 148 of the HIV-1 integrase flexible loop. *J. Biol. Chem. 281*, 461–467.
23. Dicker, I. B., Samanta, H. K., Li, A., Hong, Y., Tian, Y., Banville, J., Remillard, R. R., Walker, M. A., Langley, D. R., and Krystal, M. (2008) Changes to the HIV long terminal repeat and to HIV integrase differentially impact HIV integrase assembly, activity, and the binding of strand transfer inhibitors. *J. Biol. Chem. 282*, 31186–31196.
24. Langley, D., Samanta, H. K., Lin, Z., Walker, M. A., Krystal, M., and Dicker, I. B. (2008) The Terminal (Catalytic) Adenosine of the HIV LTR Controls the Kinetics of Binding and Dissociation of HIV Integrase Strand Transfer Inhibitors. *Biochemistry 47*, 13481–13488.
25. Dicker, I. B., Terry, B., Lin, Z., Li, Z., Bollini, S., Samanta, H. K., Gali, V., Walker, M. A., and Krystal, M. (2008) Biochemical analysis of HIV-1 integrase variants resistant to strand transfer inhibitors. *J. Biol. Chem. 283*, 23599–23609.
26. Greenwald, J., Le, V., Butler, S. L., Bushman, F. D., and Choe, S. (1999) The mobility of an HIV-1 integrase active site loop is correlated with catalytic activity. *Biochemistry 38*, 8892–8898.
27. Barreca, M. L., Lee, K. W., Chimirri, A., and Briggs, J. M. (2003) Molecular dynamics studies of the wild-type and double mutant HIV-1 integrase complexed with the 5ClTEP inhibitor: Mechanism for inhibition and drug resistance. *Biophys. J. 84*, 1450–1463.
28. Copeland, R. A., Pompliano, D. L., and Meek, T. D. (2007) Drug-target residence time and its implications for lead optimization. *Nat. Rev. Drug Discovery 5*, 730–739.
29. Hazuda, D. J., Felock, P., Witmer, M., Wolfe, A., Stillmock, K., Grobler, J. A., Espeseth, A., Gabryelski, L., Schleif, W., Blau, C., and Miller, M. D. (2000) Inhibitors of strand transfer that prevent integration and inhibit HIV-1 replication in cells. *Science 287*, 646–650.
30. Ratner, L., Haseltine, W., Patarca, R., Livak, K. J., Starcich, B., Josephs, S. F., Doran, E. R., Rafalski, J. A., Whitehorn, E. A., Baumeister, K., Ivanoff, L., Petteway, S. R., Jr., Pearson, M. L., Lautenberger, J. A., Papas, T. S., Ghrayeb, J., Chang, N. T., Gallo, R. C., and Wong-Staal, F. (1985) Complete nucleotide sequence of the AIDS virus, HTLV-III. *Nature 313*, 277–284.
31. Boros, E. E., Johns, B. A., Garvey, E. P., Koble, C. S., and Miller, W. H. (2006) Synthesis and HIV integrase strand transfer activity of 7-hydroxy[1,3]thiazolo[5,4-b]pyridin-5(4H)-ones. *Bioorg. Med. Chem. Lett. 16*, 5668–5672.
32. Morrison, J. F., and Walsh, C. T. (1988) The behavior and significance of slow-binding enzyme inhibitors. *Adv. Enzymol. Relat. Areas Mol. Biol. 61*, 201–301.
33. Nakahara, K., Wakasa-Morimoto, C., Kobayshi, M., Miki, S., Noshi, T., Seki, T., Kanamori-Koyama, M., Kawauchi, S., Suyama, A., Fujishita, T., Yoshinaga, T., Garvey, E. P., Johns, B. A., Foster, S. A., Underwood, M. R., Sato, A., and Fujiwara, T. (2008) Secondary mutations in viruses resistant to HIV-1 integrase inhibitors that restore viral infectivity and replication kinetics. *Antiviral Res.* (in press).

34. Lu, R., Limon, A., Ghory, H. Z., and Engelman, A. (2005) Genetic analyses of DNA-binding mutants in the catalytic core domain of human immunodeficiency virus type 1 integrase. *J. Virol. 79*, 2493–2505.
35. Chen, X., Tsiang, M., Yu, F., Hung, M., Jones, G. S., Zeynalzadegan, A., Qi, X., Jin, H., Kim, C. U., Swaminathan, S., and Chen, J. M. (2008) Modeling, analysis, and validation of a novel HIV integrase structure provide insights into the binding modes of potent integrase inhibitors. *J. Mol. Biol. 380*, 504–519.
36. Gonzales, B., Pajares, M. A., Hermoso, J. A., Alvarez, L., Garrido, F., Sufrin, J. R., and Sanz-Aparicio, J. (2000) The crystal structure of tetrameric methionine adenosyltransferase from rat liver reveals the methionine-binding site. *J. Mol. Biol. 300*, 363–375.
37. Pearce, F. G., and Andrews, T. J. (2003) The relationship between side reactions and slow inhibition of ribulose-bisphosphate carboxylase revealed by a loop 6 mutant of the tobacco enzyme. *J. Biol. Chem. 278*, 32526–32536.
38. Liu, Y., Stoll, V. S., Richardson, P. L., Saldivar, A., Klaus, J. L., Molla, A., Kohlbrenner, W., and Kati, W. M. (2004) Hepatitis C NS3 protease inhibition by peptidyl-α-ketoamide inhibitors: Kinetic mechanism and structure. *Arch. Biochem. Biophys. 421*, 207–216.
39. Kappor, M., Reddy, C. C., Krishnasastry, M. V., Surolia, N., and Surolia, A. (2004) Kinetic and structural analysis of the increased affinity of enoyl-ACP (acyl-carrier protein) reductase for triclosan in the presence of NAD^+. *Biochem. J. 381*, 719–724.
40. Kehlenbeck, S., Betz, U., Birkmann, A., Fast, B., Goller, A. H., Henninger, K., Lowinger, T., Marrero, D., Paessens, D., Pevzner, V., Schohe-Loop, R., Tsujishita, H., Wlder, R., Kreuter, J., Rubsamen-Waigmann, H., and Dittmer, F. (2006) Dihydroxythiophenes are novel potent inhibitors of human immunodeficiency virus integrase with a diketo acid-like pharmacophore. *J. Virol. 80*, 6883–6894.

BI802141Y